



# The geochemical behavior of Mg isotopes in the Huanghe basin, China



BaiLing Fan<sup>a,b</sup>, Zhi-Qi Zhao<sup>a,\*</sup>, FaXiang Tao<sup>a</sup>, XiaoDong Li<sup>a</sup>, ZhengHua Tao<sup>a,c</sup>, Shuang Gao<sup>a,c</sup>, MaoYong He<sup>d</sup>

<sup>a</sup> State Key Laboratory of Environmental Geochemistry, Institute of Geochemistry, Chinese Academy of Sciences, Guiyang, Guizhou 550081, China

<sup>b</sup> Guizhou Industry Polytechnic college, Guiyang, Guizhou 550008, China

<sup>c</sup> University of Chinese Academy of Sciences, Beijing 100049, China

<sup>d</sup> State Key Laboratory of Loess and Quaternary Geology, Institute of Earth Environment Chinese Academy of Sciences, Xi'an, Shanxi 710075, China

## ARTICLE INFO

### Article history:

Received 15 July 2015

Received in revised form 7 January 2016

Accepted 9 January 2016

Available online 11 January 2016

### Keywords:

Magnesium isotope

Evaporation

Secondary carbonate formation

Huanghe

## ABSTRACT

The magnesium (Mg) isotopic composition of river waters is mainly controlled by riverine Mg sources and geochemical processes. It is meaningful to characterize Mg isotope behavior for us in understanding chemical weathering and other geochemical processes, such as secondary mineral formation linked to environmental conditions. The Huanghe basin was chosen to investigate the behavior of Mg isotopes during river erosion in temperate-semiarid and arid climate. Dissolved Mg shows a wide range of  $\delta^{26}\text{Mg}$  values, ranging from  $-1.53\text{‰}$  to  $-0.11\text{‰}$ , with most values being close to  $-1.09\text{‰}$ . By comparison, most of the suspended loads are enriched in heavy Mg isotope, with  $\delta^{26}\text{Mg}$  values ranging from  $-2.00\text{‰}$  to  $-0.62\text{‰}$ , which is controlled by mineralogy. The Mg isotopic composition in the upstream is mainly determined by the mixture between carbonate and silicate sources. When the Huanghe flows through the Loess Plateau, the dissolved Mg decreased due to the dissolution of easily dissolvable phases in loess, such as  $\text{MgCl}_2$  or  $\text{MgSO}_4$ . Carbonates weathering and evaporites dissolution are the major controlling factor of the evolution of Mg isotopic composition in dissolved phase, though evaporation-related precipitation of secondary carbonates also influences the dissolved Mg isotope composition in some tributaries. The strong relationships between  $\delta^{26}\text{Mg}$  and pH, temperature, and  $\delta^{18}\text{O}$  suggest that the Mg isotope system bears significant information about the hydrogeochemical characteristics and climate conditions of the Huanghe basin.

© 2016 Elsevier B.V. All rights reserved.

## 1. Introduction

Magnesium is second only to oxygen in abundance among the rock-forming elements and its content shows much difference in different reservoirs (Brenot et al., 2008; de Villiers et al., 2005; Meybeck, 1987; Rudnick and Gao, 2003; Tipper et al., 2006b). Terrestrial materials were proved to have significant differences in their Mg isotopic composition, ranging from  $-6$  to  $1.13\text{‰}$ , and the river waters have a range from  $-2.93$  to  $0.64\text{‰}$  (Brenot et al., 2008; Geske et al., 2015a,b; Handler et al., 2009; Pogge von Strandmann et al., 2008a,b; Teng et al., 2010; Tipper et al., 2006a,b, 2008, 2012b; Young and Galy, 2004). It has been suggested that several potential factors controlling the Mg isotopic composition of river waters are mineral dissolution, incorporated/adsorbed in/onto secondary minerals, ion exchange and plant uptake. Studying the behavior of magnesium (Mg) and its isotopic composition during river erosion has the potential to provide useful information in understanding continental chemical weathering, and ultimately the carbon cycle (Berner and Berner, 2012; Berner et al., 1983; Brenot et al., 2008; de Villiers et al., 2005; Tipper et al., 2006a,b). Because the major source of riverine Mg is weathering of carbonate and silicate

rocks of the continental crust and the Mg isotopic composition differs between carbonate ( $-5.2\text{‰}$  to  $-1.1\text{‰}$ ) and silicate ( $-0.6\text{‰}$  to  $0.0\text{‰}$ ), which as a consequence, to some extent, leads to Mg isotope signatures varying widely in river systems (Galy et al., 2002; Teng et al., 2010; Tipper et al., 2006a; Young and Galy, 2004). Furthermore, riverine Mg isotopes can be influenced by secondary mineral formation (Pogge von Strandmann et al., 2008a; Wimpenny et al., 2010, 2014a), which is related to a number of environmental factors, including ion concentrations, water temperature, and pH. However, different secondary phases fractionate Mg isotopes in different ways. Some, like carbonates, which are formed under high pH conditions, appear to preferentially incorporate the light  $^{24}\text{Mg}$  isotopes (Galy et al., 2002). In contrast, others, such as clay minerals (hydroxy biotic and vermiculite) formed in lower or neutral pH conditions, appear to preferentially incorporate the heavy Mg isotopes (Tipper et al., 2006a). The variation in riverine Mg isotope composition can therefore provide significant information about the hydrogeochemical characteristics in river systems. Mg isotopes are also fractionated during plant uptake (Black et al., 2006, 2008; Kuhn et al., 2000; Ra and Kitagawa, 2007), hence the variation in the Mg isotope signature in river waters can also reflect biological processes.

The Mg isotope system has attracted more attention in the past decade because of its potential for tracing chemical weathering in river-basin scale (Brenot et al., 2008; Pogge von Strandmann et al., 2008a,b;

\* Corresponding author.

E-mail address: [zhaozhiqi@vip.skleg.cn](mailto:zhaozhiqi@vip.skleg.cn) (Z.-Q. Zhao).

Schmitt et al., 2012; Tipper et al., 2006a; Wimpenny et al., 2011). In small mono-lithological catchments, the influence of rock type is pronounced. The Mg isotope ratios of river water in carbonate-dominated catchments are generally lower than those in silicate-dominated catchments (Brenot et al., 2008; Tipper et al., 2006b). In large rivers, the dissolved Mg isotopic composition appears to be predominantly controlled by the reaction balance between the weathering of primary minerals and the formation of secondary minerals (Tipper et al., 2006a,b, 2008). Though Mg isotopes have been successfully applied to study chemical weathering in rivers (de Villiers et al., 2005; Pogge von Strandmann et al., 2008a), information from arid temperate climate watersheds is sparse. The arid temperate climate is often linked to many environmental factors such as warm temperature, higher evaporation and less rainfall, and then associated with geochemical processes. Previous studies have shown that pronounced variation in temperature, rainfall and evaporation of a region can result in changes in the Mg isotope composition in runoff/seepage water (Buhl et al., 2007; Galy et al., 2002; Riechelmann et al., 2012a,b). Hence, more work under different climate zones should be carried out to test the applicability of Mg isotopes as a tracer of environmental change and to better understand the mechanisms controlling riverine Mg isotopic composition.

The Huanghe (Yellow River) is one of the most intensely weathering systems, traversing through the thick loess plateau. The geochemistry of major ions and traditional isotopes, such as O, C and Sr isotopes has been used to ascertain regional hydrogeochemical processes, rock weathering rates and anthropogenic impacts in the Huanghe watershed (Fan et al., 2014; Wang et al., 2012; Zhang et al., 1995), while the research on Mg isotope geochemistry is rare. In the present study, the Huanghe basin was chosen to study the behavior of Mg isotopes in a temperate-arid and semiarid climate

zone and to test the potential of Mg isotopes as a tracer of lithological sources and geological processes.

## 2. Sampling and methods

### 2.1. Geological and climate background of the Huanghe basin

The Huanghe is one of 10 largest river systems over the world in terms of river length (5464 km) and sediment discharge ( $10.8 \times 10^8$  tons yr<sup>-1</sup>). It contributes about 10% of the world's annual sediment discharge (Saito et al., 2001). The Huanghe originates from mountainous areas in the northeast part of the Tibetan Plateau, with an elevation of about 5000 m. The main part of its upper and middle reaches flow through NW China (Fig. 1). After flowing through the Loess Plateau and the North China Plain, it finally enters Bohai Sea. The Huanghe basin displays complex features in lithology and topography, covered with nearly all kinds of rocks varying in age from Cambrian to Quaternary. The upstream before Lanzhou with elevations from 2000 m to 4000 m is mainly comprised of limestone, low-grade metamorphic rocks and clastic rocks interlaced with volcanic rocks and evaporites. The midstream drains through the Loess Plateau, accounting for 44% of the total watershed area. The erosion on the Loess Plateau leads to extremely high sediment yield. The downstream are underlain mainly by Tertiary–Quaternary sediments (Chen and Wang, 2006). The Huanghe basin is characterized by a temperate climate, with a mean annual temperature of between 1 and 8 °C upstream, 8–14 °C midstream, and 12–14 °C downstream, while the source area is characterized by high elevation and a cold climate. The average yearly rainfall is about 476 mm and is unevenly distributed, increasing gradually from 150 mm upstream to 900 mm midstream and downstream. The Huanghe basin

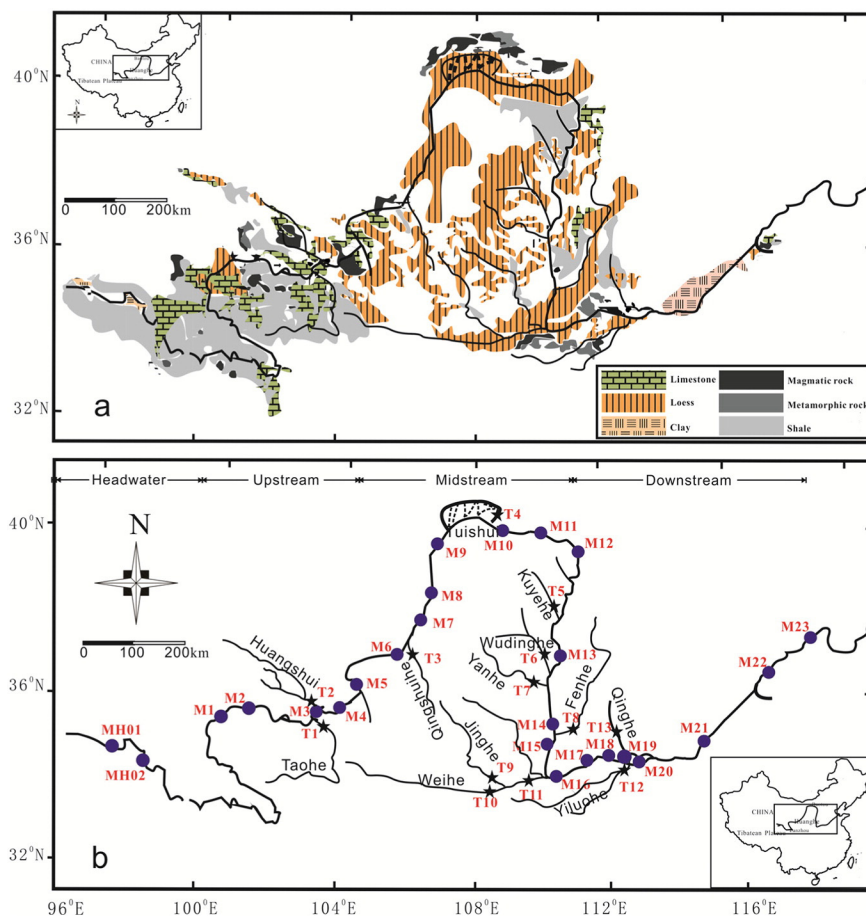


Fig. 1. Geology (a), sampling sites (b), and river flow in the Huanghe basin.

experiences particularly strong surface evaporation (about 1100 mm yearly on average, Chen and Wang, 2006).

## 2.2. Sampling

At each sampling site about 15–20 L of river water was collected along with suspended load in August 2012 along the Huanghe main channel and its main tributaries (see Fig. 1b). The T and pH were measured in the field using Multi parameter water probe meters. The water samples were filtered within a few hours after collection through 0.45  $\mu\text{M}$  cellulose acetate filters, and then the alkalinity was determined with the Gran titration method. Water samples for analysis of Mg isotopes were immediately acidified to pH 2 with thermally distilled (TD)  $\text{HNO}_3$ . After return to the laboratory, the suspended material was dried at 60  $^\circ\text{C}$ .

## 2.3. Analytical methods

Magnesium was separated from the sample matrix by ion exchange chromatography. The analytic methods employed in this study broadly follow those employed in previous studies (Chang et al., 2002; Teng et al., 2007). Bulk suspended load were dissolved in a HF– $\text{HNO}_3$  acid mixture, and were passed through at least two cation exchange columns (AG50W-X8 resin) eluted with 1 N  $\text{HNO}_3$ . River waters were first dried in Teflon beakers at 80  $^\circ\text{C}$ , and then dissolved twice in a mixture of concentrated  $\text{HNO}_3$  and HF to degrade any organic matter before converting to a nitrate salt ready for ion exchange separation. The total blank and the recovery of this procedure was  $\sim 4$  ng and  $>99\%$ . Mg isotope ratios were measured by Neptune MC-ICP-MS using the standard–sample bracketing (SSB) method in the State Key Laboratory of Loess and Quaternary Geology. Results were reported relative to DSM3 (Dead Sea Magnesium, a reference material distributed by Cambridge University) in the conventional delta notation:

$$\delta^{25}\text{Mg}(\text{‰}) = \left\{ \left( \frac{^{25}\text{Mg}/^{24}\text{Mg}}{\text{sample}} / \left( \frac{^{25}\text{Mg}/^{24}\text{Mg}}{\text{DSM3}} - 1 \right) \right) \times 1000 \right.$$

$$\delta^{26}\text{Mg}(\text{‰}) = \left\{ \left( \frac{^{26}\text{Mg}/^{24}\text{Mg}}{\text{sample}} / \left( \frac{^{26}\text{Mg}/^{24}\text{Mg}}{\text{DSM3}} - 1 \right) \right) \times 1000 \right.$$

The Mg concentration of the sample was adjusted to the same concentration ( $\pm 10\%$ ) as the standard, typically 0.1–0.3 mg/L. The mean long term reproducibility ( $\delta^{26}\text{Mg}$ ) was about 0.06 ‰, evaluated by the repeat analysis of mono–elemental standards, SRM980 and DSM3. At the same time, to test the potential fractionation of Mg isotopes during chemical separation, a synthetic multi–elemental standard was treated using the same chemical procedure and measured by the same methods. The results show that the chemical–separation fractionation of  $\delta^{26}\text{Mg}$  was 0.06 ‰, similar to the machine reproducibility. Using the above chemical procedure and measuring methods, a seawater sample from the South China Sea and an international rock reference, BCR-1, were analyzed. The average  $\delta^{26}\text{Mg}$  value of the seawater was

**Table 1**

Concentrations of Ca, Mg and magnesium isotope compositions for the suspended loads of the Huanghe River, and magnesium isotope composition of BCR-1.

Sample	Ca (wt.%)	Mg (wt.%)	$\delta^{25}\text{Mg}$ (‰) $\pm 2\sigma$	$\delta^{26}\text{Mg}$ (‰) $\pm 2\sigma$	N
M8	4.50	0.45	$-1.07 \pm 0.04$	$-2.00 \pm 0.08$	2
M10	4.39	0.92	$-0.64 \pm 0.02$	$-1.20 \pm 0.00$	2
M11	10.03	1.16	$-0.78 \pm 0.1$	$-1.44 \pm 0.08$	2
M13	4.59	1.87	$-0.54 \pm 0.00$	$-0.94 \pm 0.03$	2
M16	7.52	0.5	$-0.38 \pm 0.09$	$-0.62 \pm 0.1$	2
M17	7.41	1.35	$-0.53 \pm 0.05$	$-0.94 \pm 0.36$	3
M19	6.7	1.5	$-0.39 \pm 0.12$	$-0.68 \pm 0.03$	2
M22	4.36	1.02	$-0.37 \pm 0.07$	$-0.68 \pm 0.13$	2
M23	3.86	0.84	$-0.48 \pm 0.04$	$-0.87 \pm 0.03$	3
BCR-1			$-0.13 \pm 0.02$	$-0.25 \pm 0.04$	2

$-0.85 \text{‰} \pm 0.04$ . BCR-1 has a  $\delta^{26}\text{Mg}$  value of  $-0.25 \text{‰} \pm 0.04$  (Table 1). These values are identical to those reported in previous studies within uncertainty (Foster et al., 2010; Ling et al., 2011; Young and Galy, 2004).

## 3. Results

### 3.1. Physicochemical properties of river water

The pH of river water samples range from 7.4 to 9.8, with an average value of 8.0. The headwater tributary (MH02) and tributary (T4) exhibit anomalously high pH; The water temperature ranged from 9.6 to 29.1  $^\circ\text{C}$ , and increased from upstream to downstream (Fan et al., 2014). Calcite saturation index (CSI) and dolomite saturation index (DSI) were calculated based on pH, temperature, and the concentrations of measured anions and cations reported by Fan et al. (2014) using the program of Zeebe and Wolf-Gladrow and the thermodynamic database provided with it available at <http://www.awi-bremerhaven.de>. These results indicate that all the samples except for M3 are supersaturated with calcite, having CSI ranging from 0.02 to 1.3, and, with the exception of M1, M3 and M19, all other samples are supersaturated with dolomite, having DSI ranging from 0.4 to 3.8 (Table 2).

### 3.2. Major element concentrations

#### 3.2.1. Suspended load

The chemical composition of the suspended load is different from that of primary source. The suspended load has Mg concentrations in the range of 0.45–1.87 wt.%, and Ca concentrations in the range of 3.86–10.03 wt.% (Table 1); Ca/Mg ratios vary from 1.47 to 9.13, 4.03 on average. Ca/Mg ratios of loess samples from Loess Plateau were reported in the range of 0.61 to 5.17, 2.49 on average (Huang et al., 2013).

#### 3.2.2. Dissolved load

The results of water chemistry and oxygen isotopic compositions of the water samples were reported in our earlier research (Fan et al., 2014). Mg concentrations range from 663 to 23,100  $\mu\text{M/L}$ , which are clearly higher than those in Moselle rivers (27–4847  $\mu\text{M/L}$ , Brenot et al., 2008), Han River (35.9–353  $\mu\text{M/L}$ , Lee et al., 2014), Iceland rivers (13.2–97.6  $\mu\text{M/L}$ , Pogge von Strandmann et al., 2008a) and Mackenzie rivers (61–930  $\mu\text{M/L}$ , Tipper et al., 2012a). For all water samples, the Mg concentrations are well correlated with Na ( $R^2 = 0.98$ ), Cl ( $R^2 = 0.91$ ) and  $\text{SO}_4$  ( $R^2 = 0.92$ ) concentrations, but there is poor relationship between Mg and the other major elements. This indicates that evaporites are likely to be an important source of Mg in the Huanghe River basin.

### 3.3. Magnesium isotopic compositions

The  $\delta^{26}\text{Mg}$  value of the suspended load ranged from  $-2.0$  to  $-0.6\text{‰}$  (Table 1), showing an increasing trend from upstream to downstream. The suspended load sampled at Wuhai (M8) has the lowest Mg isotopic composition, falling within the range of carbonates ( $-1.1\text{‰}$  to  $-5.2\text{‰}$ , Tipper et al., 2006b; Young and Galy, 2004).

The dissolved Mg of the Huanghe basin present a wide range of  $\delta^{26}\text{Mg}$  values, extending from  $-1.53\text{‰}$  to  $-0.11\text{‰}$ , whereas the Huanghe main channel contains a narrow range from  $-1.27\text{‰}$  to  $-0.85\text{‰}$ , with the majority of the river waters featuring compositions around  $-1.10\text{‰}$ . Tributaries of the Huanghe have a range of  $\delta^{26}\text{Mg}$  values from  $-1.53\text{‰}$  to  $-0.11\text{‰}$  (Table 2). The average value is indistinguishable from that of the global average of rivers ( $-1.09\text{‰}$ , Tipper et al., 2006b), but significant lower than that of most of suspended load, and loess (on average,  $-0.62\text{‰}$ ) sampled in Chinese Loess Plateau (Huang et al., 2013; Wimpenny et al., 2014b; Young and Galy, 2004). The highest value ( $-0.11\text{‰}$ ) was found in one headwater tributary MH02. The tributaries T12

**Table 2**  
Mg isotopic composition of the dissolved load of the Huanghe River.

	Sample	Location	Latitude	Longitude	CSI	DSI	$\delta^{26}\text{Mg}$ (‰) $\pm 2\sigma$	$\delta^{25}\text{Mg}$	N
Headwater	MH01	Lake Zhaling	35°05'42.2"	97°54'24.78"	0.874	1.715	$-0.91 \pm 0.05$	$-0.48 \pm 0.06$	2
	MH02	Maduo	34°49'46.58"	98°20'38.49"	1.111	3.597	$-0.11 \pm 0.05$	$-0.06 \pm 0.01$	2
Upstream	M1	Tangnaihai	35°30'03.96"	100°10'00.98"	0.039	-0.169	$-0.85 \pm 0.11$	$-0.44 \pm 0.02$	3
	M2	Guide	36°03'37.72"	101°27'08.37"	0.558	0.726	$-0.85 \pm 0.03$	$-0.41 \pm 0.11$	2
	M3	Lanzhou	35°55'19.09"	103°20'43.38"	-0.068	-0.361	$-1.04 \pm 0.06$	$-0.54 \pm 0.12$	2
	M4	Lanzhou	36°10'05.72"	103°26'06.84"	0.549	0.817	$-1.08 \pm 0.04$	$-0.56 \pm 0.08$	2
	M5	Lanzhou	36°03'30.32"	103°59'20.42"	0.611	0.968	$-1.14 \pm 0.04$	$-0.59 \pm 0.06$	2
Midstream	M6	Zhongwei	37°29'01.26"	105°11'12.97"	0.752	1.283	$-1.09 \pm 0.08$	$-0.57 \pm 0.06$	2
	M7	Yingchuan	38°20'49.32"	106°24'03.30"	0.473	0.854	$-1.00 \pm 0.04$	$-0.51 \pm 0.03$	2
	M8	Wuhai	39°15'41.09"	106°47'34.71"	0.3	0.602	$-0.98 \pm 0.06$	$-0.51 \pm 0.02$	2
	M9	Wuhai	40°15'41.97"	107°01'23.88"	0.553	1.033	$-1.03 \pm 0.04$	$-0.54 \pm 0.10$	2
	M10	Baotou	40°36'29.09"	108°46'27.51"	0.826	1.616	$-1.05 \pm 0.07$	$-0.55 \pm 0.03$	2
	M11	Baotou	40°29'10.03"	109°41'29.17"	0.746	1.462	$-0.95 \pm 0.15$	$-0.51 \pm 0.08$	2
	M12	Tuoketuo	40°13'00.33"	111°10'46.57"	0.693	1.351	$-1.14 \pm 0.00$	$-0.59 \pm 0.07$	2
	M13	Wupu	37°26'46.04"	110°42'05.10"	0.358	0.645	$-1.25 \pm 0.04$	$-0.66 \pm 0.06$	2
	M14	Hukou	36°08'49.09"	110°26'36.73"	0.218	0.493	$-1.03 \pm 0.10$	$-0.53 \pm 0.09$	2
	M15	Qiachuan	35°08'08"	110°21'57.89"	0.546	0.976	$-1.13 \pm 0.00$	$-0.59 \pm 0.01$	2
	M16	Tongguan	34°36'16.5"	110°19'36.14"	0.335	0.629	$-1.16 \pm 0.12$	$-0.60 \pm 0.03$	2
Downstream	M17	Mianchi	34°53'33.47"	111°36'11.83"	0.307	0.751	$-1.27 \pm 0.1$	$-0.66 \pm 0.05$	2
	M18	Xiaolangdi	35°04'18.48"	111°48'55.11"	0.213	0.41	$-1.19 \pm 0.03$	$-0.60 \pm 0.09$	2
	M19	Xiaolangdi	34°55'17.87"	112°24'20.9"	0.41	0.805	$-1.23 \pm 0.00$	$-0.62 \pm 0.07$	2
	M20	Huayuankou	34°54'32.66"	113°42'06.75"	0.288	0.547	$-1.23 \pm 0.07$	$-0.68 \pm 0.03$	2
	M21	Gaocun	35°22'59.22"	115°04'45.73"	0.015	-0.001	$-1.17 \pm 0.00$	$-0.63 \pm 0.02$	2
	M22	Jinan	36°44'08.79"	116°55'32.1"	0.218	0.41	$-1.17 \pm 0.01$	$-0.59 \pm 0.20$	2
	M23	Dongying	37°29'24.94"	118°15'18.98"	0.527	1.023	$-1.13 \pm 0.07$	$-0.58 \pm 0.04$	2
	Tributaries	T1	Taohe	35°55'20.8"	103°20'51.64"	0.705	1.151	$-1.14 \pm 0.06$	$-0.60 \pm 0.00$
T2		Huangshui	36°10'06.31"	103°13'08.68"	0.602	0.945	$-1.16 \pm 0.00$	$-0.60 \pm 0.02$	2
T3		Qingshuihe	37°11'20.53"	105°47'19.39"	0.98	2.432	$-1.01 \pm 0.26$	$-0.52 \pm 0.06$	2
T4		Tuishui	40°49'43.12"	108°45'45.21"	1.38	3.875	$-0.77 \pm 0.04$	$-0.40 \pm 0.04$	2
T5		Kuyehe	39°00'20.7"	110°26'28.32"	0.643	1.086	$-1.08 \pm 0.07$	$-0.56 \pm 0.04$	2
T6		Wudinghe	37°28'46.52"	110°17'01.21"	0.576	1.291	$-1.16 \pm 0.04$	$-0.60 \pm 0.04$	2
T7		Yanhe	36°32'23.51"	110°05'49.80"	0.196	0.458	$-1.34 \pm 0.05$	$-0.70 \pm 0.03$	2
T8		Fenhe	35°33'26.69"	110°42'16.22"	0.388	0.635	$-1.42 \pm 0.00$	$-0.74 \pm 0.12$	2
T9		Jinghe	34°26'28"	109°0'7"	0.318	0.487	$-1.25 \pm 0.05$	$-0.65 \pm 0.08$	2
T10		Weihe	34°27'40.13"	108°58'33.28"	0.364	0.998	$-1.23 \pm 0.04$	$-0.64 \pm 0.16$	2
T11		Weihe	34°37'46.66"	109°59'38.69"	0.097	0.278	$-1.19 \pm 0.07$	$-0.62 \pm 0.14$	2
T12		Yiluohe	34°48'27.56"	113°02'02.53"	0.506	0.82	$-1.53 \pm 0.08$	$-0.80 \pm 0.06$	3
T13		Qinghe	35°02'47.87"	113°05'35.85"	0.503	0.773	$-1.51 \pm 0.09$	$-0.79 \pm 0.02$	2

(Yiluohe) and T13 (Qinghe) from the most downstream of the Huanghe basin have the lowest  $\delta^{26}\text{Mg}$  values. The  $\delta^{26}\text{Mg}$  value of headwater sample MH01 ( $-0.91$  ‰) is close to the reported values

of glacial ice and seawater ( $-0.83$  ‰, Wimpenny et al., 2011), and similar to those of other Asian rivers draining the Himalayan-Tibetan-Plateau (HTP) region (Tipper et al., 2006b).

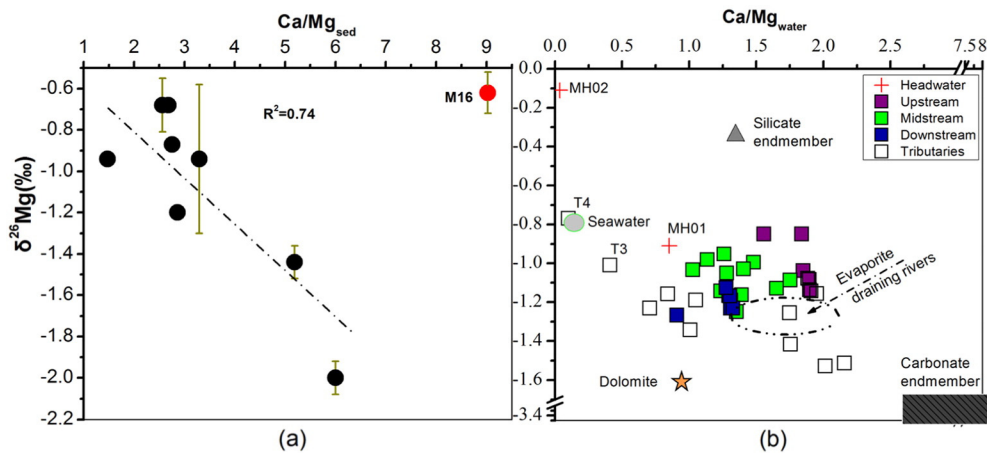


**Fig. 2.** Mg isotope compositions of suspended sediment (a) and dissolved load (b) from the Huanghe River versus the molar Ca/Mg ratio.  $\delta^{26}\text{Mg}$  values of seawater are taken from Pogge von Strandmann et al. (2008a). The  $\delta^{26}\text{Mg}$  values of carbonates and silicates data are from Young and Galy. (2004) and Tipper et al. (2006b); The data of evaporites draining rivers are from Brenot et al. (2008).

4. Discussion

4.1. Mineralogical control on  $\delta^{26}\text{Mg}$  of suspended load

There is a strong linear covariation ( $r = -0.9$ ) between  $\delta^{26}\text{Mg}$  value and Ca/Mg ratio for the suspended load, with the exception of the M16 (Fig. 2a). This is consistent with a mixture of two main phases, such as silicate characterized by high  $\delta^{26}\text{Mg}$  and low Ca/Mg ratio, and carbonate with low  $\delta^{26}\text{Mg}$  and high Ca/Mg ratio. There is therefore a strong mineralogical control on the  $\delta^{26}\text{Mg}$  of the sediment load, similar to that observed in the Mackenzie Basin for  $\delta^{26}\text{Mg}$  in the suspended load (Tipper et al., 2012a). According to XRD analysis, the sample M16 has high content of feldspar, which could be responsible for the high Ca/Mg ratio in it, for some feldspar, such as anorthite, is enriched in Ca and depleted in Mg. Further, most of Mg isotopic compositions in suspended load fall within the range of Chinese loess values ( $-0.93$  to  $-0.41$  ‰, Huang et al., 2013; Wimpenny et al., 2014b), consistent with the fact that suspended load in Huanghe is mainly originated from physical erosion in Loess Plateau (Zhang et al., 1995).

4.2. Controlling factors of dissolved Mg isotopic composition

The  $\delta^{26}\text{Mg}$  of river waters in the mainstream shows a decreasing trend from upstream to downstream (Fig. 3). Generally, the waters in tributaries have much lower  $\delta^{26}\text{Mg}$  value than mainstream waters. And the dissolved load has a lower  $\delta^{26}\text{Mg}$  value than the solid phases. The potential causes for this isotope variation will be discussed in the following sections.

4.2.1. Precipitation

Precipitation is the most common potential input to the surface environment, it must be considered. In present study as we did not collect precipitation sample, we presumed that precipitation has the same Mg

isotope composition as the seawater averaged on  $-0.84$  ‰ (Bolou-Bi et al., 2010; Tipper et al., 2010, 2012b; Riechelmann et al., 2012a,b). In theory, Mg isotopic composition of the Huanghe waters could be produced simply by the mixture of precipitation and evaporite/carbonate sources (Fig. 2b). While precipitation input is unlikely pronounced, calculations based on dissolved  $\text{F}^-$  concentrations (according to Fan et al., 2014) suggest that the magnitude of this precipitation input is too low to account for the dissolved Mg composition. As only less than 5% of the dissolved Mg in these rivers can be derived from precipitation.

4.2.2. Lithological control

As discussed in Fan et al. (2014), chemical composition of the Huanghe water is mainly controlled by carbonates weathering and evaporites dissolution. Hence, it might be expected that there is a lithological control on both Mg concentrations and  $\delta^{26}\text{Mg}$  values. As precipitation contribution is minor,  $\delta^{26}\text{Mg}$  values in the Huanghe water also can be modeled as three-component mixing between Mg sourced from silicate and dolomite, and Mg-bearing calcite. Carbonate weathering is of primary importance in controlling the water chemistry in upstream, with Ca and  $\text{HCO}_3^-$  as the dominant dissolved ions (Fan et al., 2014). However, the water  $\delta^{26}\text{Mg}$  values ( $-1.14$  ‰ to  $-0.85$  ‰) are clearly higher than those draining carbonate rocks ( $-2.50$  ‰ to  $-1.37$  ‰, Tipper et al., 2006b), but much lower than the rivers draining silicate rocks ( $-1.2$  ‰ to  $-0.54$  ‰, Brenot et al., 2008; Lee et al., 2014; Tipper et al., 2006b). This can be explained by a straightforward mixing of silicate and carbonates sources (Fig. 2b). Assuming that evaporites contribution is neglected (evidenced by the negative  $\delta^{34}\text{S}$  values for the most upstream waters) and carbonates has a  $\delta^{26}\text{Mg}$  value of  $-3.2$  ‰ and silicate with a value of  $-0.22$  ‰ (Tipper et al., 2006b), mass-balance calculations show that weathering of carbonates supplies  $\sim 24\%$  of the Mg in the rivers, while weathering of silicates supplies the remaining  $\sim 76\%$ . This ratio is consistent with the observation

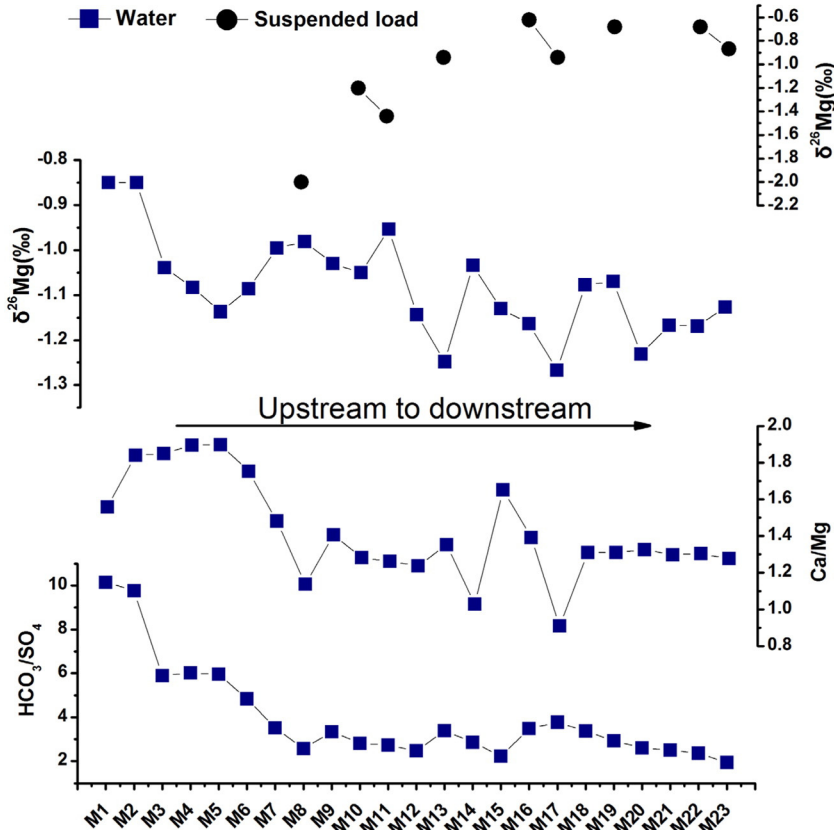


Fig. 3. Mg isotope compositions of suspended sediment and dissolved load, and Ca/Mg and  $\text{HCO}_3^-/\text{SO}_4$  molar ratios for river samples of the Huanghe main channel.

that most Mg in sediment from Chinese Loess Plateau is contained in the silicates other than carbonates (Yokoo et al., 2004).

Overall, the Huanghe waters in the midstream and downstream nearly inherited the Mg isotopic composition for upstream (Fig. 2b), consistent with the fact that the upper Huanghe supplies ~80% of the TDS flux at the mouth of the Huanghe (Wu et al., 2005). Nevertheless, when Huanghe drains over Central Loess Plateau, there is a ~0.3‰ decrease in dissolved  $\delta^{26}\text{Mg}$  values of the main channel (Fig. 3). The average  $\delta^{26}\text{Mg}$  value of river waters in the mainstream (−1.08‰) is significant lower than that of the Chinese loess (on average, −0.62‰, Huang et al., 2013; Wimpenny et al., 2014b), and most of suspended load (Fig. 3), whilst molar Ca/Mg ratios are also lower than that in these two phases. The leaching experiments of Chinese loess indicated that loess was composed of silicates, carbonates and evaporites which displayed distinct solubility, and these phases were believed to possess characteristic  $\delta^{26}\text{Mg}$  (Yokoo et al., 2004; Wimpenny et al., 2014b). Therefore, the decrease in dissolved  $\delta^{26}\text{Mg}$  values might be the result of incongruent dissolution of loess. This suggests that, in addition to having relatively low  $\delta^{26}\text{Mg}$  values, any sources in loess must also contribute lower Ca/Mg ratios to the dissolved solute. Carbonate is a major mineral component in loess, accounting for 5–20% of the total minerals present in it (Zhang et al., 1990), and carbonate minerals are generally enriched in isotopically light Mg (Geske et al., 2015a; Tipper et al., 2006b; Young and Galy, 2004). Hence, it is plausible that the decrease in the dissolved  $\delta^{26}\text{Mg}$  value in the main channel is the result of carbonate dissolution in loess. However, this is inconsistent with the fact that there is a decreasing trend in Ca/Mg ratios from upstream to downstream (Fig. 3), and cannot account for the lower Ca/Mg values relative to loess, because carbonates are generally characterized by relatively high Ca/Mg ratio (Dessert et al., 2003). The leachate of Chinese loess was isotopically light and had high Ca/Mg ratios (>10) (Wimpenny et al., 2014b) which also supports this. However, except for three samples (MH02, T3 and T4), carbonate weathering seems to have a great influence on the  $\delta^{26}\text{Mg}$  of major tributaries, in particular for the most downstream tributaries (T12 and T13) which are characterized by lower  $\delta^{26}\text{Mg}$  values, and meanwhile feature the highest Ca/Mg ratios (Fig. 2b).

Another potential source of isotopically light Mg is evaporites that have been observed to drive rivers to lower  $\delta^{26}\text{Mg}$  values from −1.4‰ to −1.2‰ (Brenot et al., 2008) relative to global average value of rivers. Evaporites concentration in Chinese loess has been shown to generally vary between 5 and 10% (Zhang et al., 1990). Moreover, the dissolution rate of evaporites is 40–80 times higher than granites, and 4–7 times higher than carbonates, according to the estimation of Meybeck (1987). As a consequence, the dissolution of evaporites in loess could be responsible for the lower  $\delta^{26}\text{Mg}$  values observed in downstream samples, which is also evidenced by the good relationship between Mg, and Cl and  $\text{SO}_4$ . Previous studies have shown that some Mg present in evaporites as  $\text{MgCl}_2$  or  $\text{MgSO}_4$  (Noh et al., 2009; Wu et al., 2005), and  $\text{MgCl}_2$  is characterized by a Mg isotope lower value of −1.63‰ (Wimpenny et al., 2014a), so the dissolution of evaporites can impart the water with low Ca/Mg and the light Mg isotope. From upstream to downstream, the decrease of molar  $\text{HCO}_3/\text{SO}_4$  or  $\text{HCO}_3/\text{Cl}$  and Ca/Mg ratio further suggest that there is an increasing contribution from evaporites dissolution (Fig. 3). It is therefore indicative of some Mg presenting as easily dissolution phases in loess relative to Ca, such as  $\text{MgCl}_2$  or  $\text{MgSO}_4$ , supported by the relatively high Ca/Mg ratio in suspended load (representative of the loess being weathered because of the low degree of weathering) relative to loess. Ultimately, the input of Mg from evaporites dissolution could be responsible for the ~0.3‰ decrease for  $\delta^{26}\text{Mg}$  values in the Huanghe main channel, in agreement with the fact that there is an increasing contribution of evaporites dissolution from upstream to downstream (Fan et al., 2014). Further, Mg isotopic compositions and Ca/Mg ratios in some tributaries (T1, T2, T5, T8 and T9) are similar to the rivers draining evaporites. These tributaries were also found to be either with evaporites

wide spread or draining loess-covered areas (Wu et al., 2005). In addition, most samples shows negative relationship between  $\delta^{26}\text{Mg}$  and  $\delta^{34}\text{S}$  values (unpublished data), which further indicates that the influence from evaporites dissolution is significant, as  $\delta^{34}\text{S}$  has been previously used as a tracer of evaporites (evaporites often feature high  $\delta^{34}\text{S}$  value) (Fig. 4).

#### 4.2.3. Evaporation-related secondary minerals formation

Previous studies have shown that Mg isotopic composition in rivers can be affected by the formation of secondary carbonate and clay mineral (Buhlt et al., 2009; Galy et al., 2002; Pogge von Strandmann et al., 2008a; Saulnier et al., 2012; Tipper et al., 2006a,b, 2008, 2012b; Wimpenny et al., 2010, 2014a). As silicate weathering is not important in the Huanghe basin (Fan et al., 2014), the accompanying product consisting of clay minerals is minor. While the temperate-arid climate and relatively high alkalinity of the Huanghe waters are favorable for the precipitation of secondary carbonate minerals such as calcite, and dolomite (English et al., 2000; Geske et al., 2015b; Jacobson et al., 2002; Mavromatis et al., 2014a; Tipper et al., 2006a) as evaporation is intense in the temperate-arid climate, Ca and Mg concentrations are generally high, and carbonates formation is highly dependent on pH. Even if it is difficult to determine whether the secondary carbonate actually occurs in the rivers, it could possible occur as suggested by previous studies (Brenot et al., 2008; Tipper et al., 2006a). Carbonate is always enriched in light Mg isotopes, so the formation of secondary carbonate in river system has the potential to increase the  $\delta^{26}\text{Mg}$  values in waters particularly for Mg-rich minerals, such as dolomite (Galy et al., 2002; Riechelmann et al., 2012a,b; Immenhauser et al., 2010; Kisakurek et al., 2009; Li et al., 2012; Mavromatis et al., 2012, 2014a; Rustad et al., 2010; Schauble, 2011). Given that the fractionation occurs during formation of secondary carbonate in the Huanghe system, the good relationship between  $\delta^{26}\text{Mg}$  and CSI and DSI is expected. As shown in Fig. 5, there is no systematic variation between  $\delta^{26}\text{Mg}$  and CSI or DSI in the Huanghe main channel. In contrast, the good positive relationships between  $\delta^{26}\text{Mg}$  and CSI and DSI are observed for tributaries. These results indicate that secondary carbonates formation is, at best, a secondary role in controlling the Mg isotope signature in the Huanghe main channel, whereas for some tributaries, this process is significant. If this is the case, it can be responsible for the samples which do not fall within the envelope described by silicate and carbonates end-members, in particular for MH02 which is characterized by anomalously high  $\delta^{26}\text{Mg}$  value and the highest CSI and DSI. The  $\delta^{26}\text{Mg}$  value for MH02 (−0.11‰) is within the range of −0.14‰ to 0.17‰ for alkaline lake waters (Mavromatis et al., 2012; Shirokova et al., 2013). The precipitation of Mg-bearing carbonates was observed in this alkaline lake, and the corresponding waters are characterized by higher Mg isotope

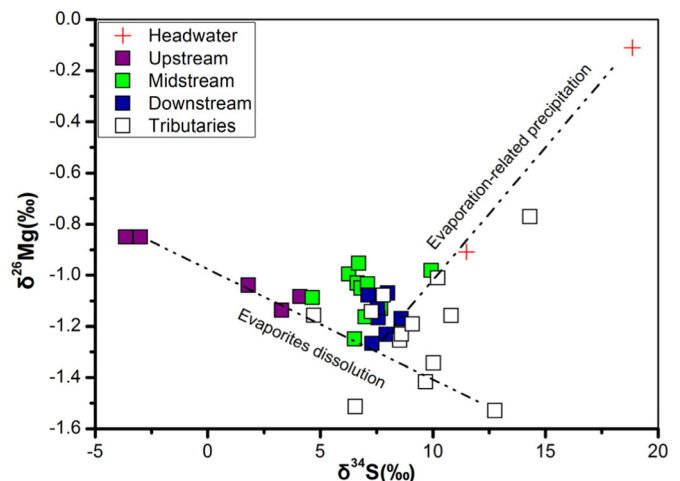
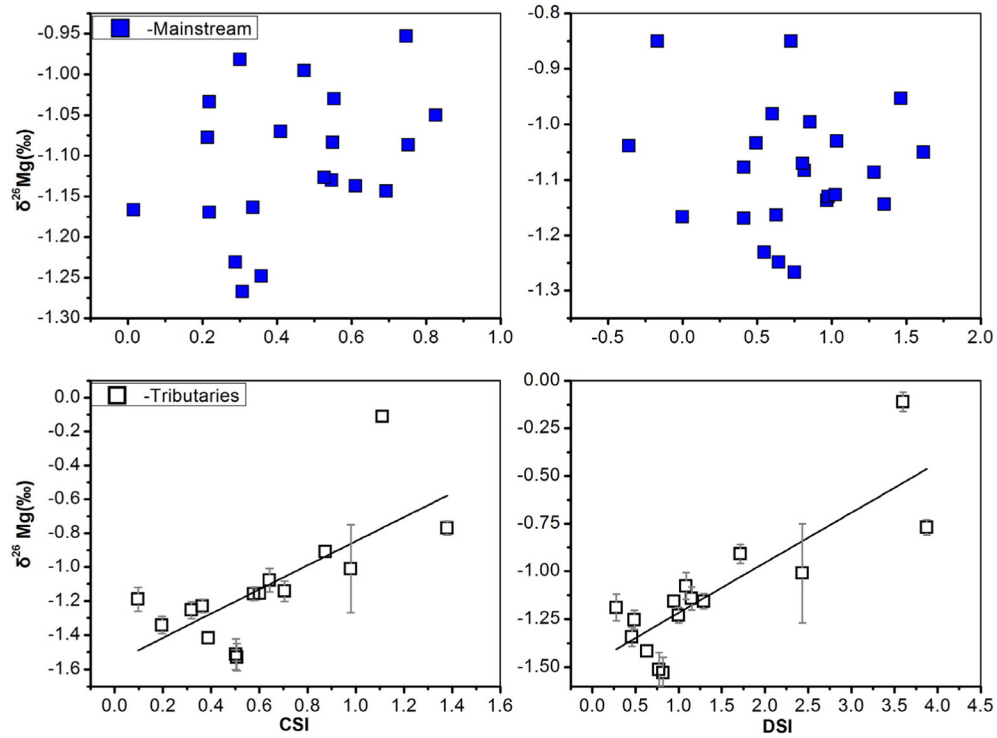


Fig. 4. Plots showing variations of  $\delta^{26}\text{Mg}$  with  $\delta^{34}\text{S}$  for Huanghe river samples.



**Fig. 5.** Plots showing variations of  $\delta^{26}\text{Mg}$  with CSI (calcite saturation index) and DSI (dolomite saturation index) in the Huanghe mainstream and its major tributaries. The good relationship between  $\delta^{26}\text{Mg}$ , and CSI ( $r = 0.69$ ) and DSI ( $r = 0.81$ ) in the tributaries reveal that the formation of secondary carbonates has a significant effect on the riverine Mg isotopic composition.

ratios (Shirokova et al., 2013). In the present study area, these waters are also characterized by relatively low Ca/Mg ratios, particularly for water samples MH02 and T4 (0.04, 0.10), implying that carbonate precipitation have occurred in this region. Following a Rayleigh law, 10% of Mg would be precipitated in sample MH02, and 2% in sample T4 (with a corresponding  $\Delta^{26}\text{Mg}_{\text{calcite-solution}} = -6\text{‰}$ , Li et al., 2012, 2015), and Mg partition coefficient between carbonates and the solution ( $K_d$ ) of 0.004, 0.007 for MH02 and T4 were measured during carbonate precipitation; While given that  $\Delta^{26}\text{Mg}_{\text{dolomite-solution}} = -2.6\text{‰}$  (reported by Mavromatis et al., 2014a), 27% of Mg would be precipitated in sample MH02, and 5% in sample T4. And the  $K_d$  values were determined at 0.012, 0.003 for MH02 and T4, respectively. Whatever,  $K_d$  values determined in this study is lower than experimental data ( $0.01 \leq K_d \leq 0.03$ ) at 25 °C (Mavromatis et al., 2013). This discrepancy might be resulted from different fluid condition between our study site and the controlled experimental setting, such as temperature.

It can be inferred that the high alkalinity water is always enriched in isotopically heavy Mg isotopes, due to precipitation of Mg-bearing carbonates. This conclusion might support the hypothesis that seawater always being isotopically heavier relative to that of global average of rivers ( $-1.09\text{‰}$ ) is a result of dolomite precipitation (Tipper et al., 2006b).

Oxygen isotopes of rivers often reflect the evaporation intensity in catchment. A good relationship can be found between  $\delta^{26}\text{Mg}$  and  $\delta^{18}\text{O}$  ( $r = 0.64$ ,  $p < 0.02$ ) for the Huanghe main tributaries, excluding T12 and T13 for which calcite dissolution is predominant (Fig. 6a). This again indicates that the high  $\delta^{26}\text{Mg}$  values are associated with evaporation-related Mg loss, e.g., carbonate precipitation, because the temperate-arid condition not only can lead to the precipitation of calcite or dolomite causing an enrichment of the water in the heavy Mg isotope, but also can drive  $\delta^{18}\text{O}$  towards high values. Further, the positive correlation between  $\delta^{26}\text{Mg}$  and  $\delta^{34}\text{S}$  values for some water samples reflects that evaporation related secondary carbonate formation did occur (Fig. 4). In addition, good relationships between  $\delta^{26}\text{Mg}$ , and water pH ( $r = 0.90$ ,  $p < 0.01$ ) and temperature ( $T$ ) ( $r = -0.71$ ,  $p < 0.01$ ) (Fig. 6b,c) are observed. However, laboratory experiments have shown that Mg isotope fractionation during precipitation of inorganic carbonates was found to be independent of  $T$  in solutions (Mavromatis et al., 2012; Shirokova et al., 2013). This contrasting observation indicates that  $T$  in this study might be not connected with fractionation of Mg isotope but be related to the supersaturation of the solution. High pH is expected to reduce the undersaturation of carbonates, which promotes the formation of secondary carbonates.

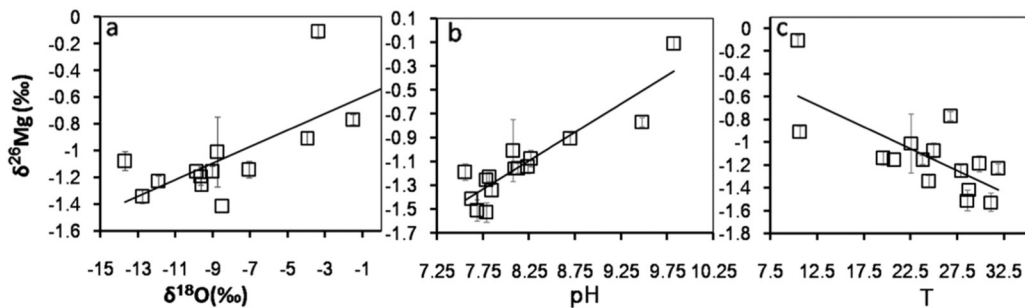


**Fig. 6.** The correlation between  $\delta^{26}\text{Mg}$  and  $\delta^{18}\text{O}$  (a) for Huanghe main tributaries including two headwater tributaries (MH01, MH02), but excluding the most downstream rivers (T12, T13);  $\delta^{26}\text{Mg}$  as a function of pH (b) and  $T$  (c) for all the tributaries.

Therefore a good positive relationship is observed between  $\delta^{26}\text{Mg}$  and pH.

#### 4.2.4. Biological Control

Magnesium is an essential nutrient for plants, exerting an important role in photosynthetic processes. Experiments have shown that vegetation may be highly enriched in Mg and heavier Mg isotopes, which potentially drives the Mg isotope composition of nutrient solution towards low  $\delta^{26}\text{Mg}$  values (Black et al., 2006, 2008; Bolou-Bi et al., 2010; Ra and Kitagawa, 2007; Ra et al., 2010; Tipper et al., 2010). And previous researches indicated that uptake of isotopically heavier Mg by plant, or decay and recycling of plant could influence the riverine Mg isotope signature (Opfergelt et al., 2014; Mavromatis et al., 2014b). However, the influence of plants on Mg isotopic compositions of river waters with strong gradient in vegetation was not observed (Tipper et al., 2008). In any case, such an affect could not be a major factor controlling the Huanghe rivers Mg isotope composition, as the level of vegetation cover in the Chinese Loess Plateau is small. Further, given that biological activity is important, the pH of waters in the downstream with relative high level of vegetation cover should be modified significantly (Shirokova et al., 2013), but what was not observed.

#### 4.2.5. Anthropogenic inputs

The area irrigated for agriculture (wheat, maize, soybean) accounts for ~15% of the downstream, while it is only 0.3% for the upper drainage basin (Wu et al., 2005). Corresponding, it is necessary to evaluate the anthropogenic impact on the  $\delta^{26}\text{Mg}$  of the Huanghe downstream. The Mg isotope composition of the fertilizers has not yet been measured. A recent study has shown that the Mg isotope composition of fertilizers ranged from  $-1.48\%$  for chemical fertilizers to  $-0.75\%$  for organic fertilizers (Lee et al., 2014). The  $\delta^{26}\text{Mg}$  values for water samples are between those of chemical and organic fertilizers, which could imply that fertilizers affect river water. However, the lack of a correlation between  $\text{NO}_3$  which is most likely of anthropogenic origin, and  $\delta^{26}\text{Mg}$  suggests that anthropogenic input should not be an important controlling factor for the riverine Mg. In addition, the S isotope evidence also indicates that the influence of anthropogenic inputs should be minor, the relationship between  $\delta^{26}\text{Mg}$  and  $\delta^{34}\text{S}$  reflects the significant influence from evaporites dissolution. This is in good agreement with the observations in previous study (Fan et al., 2014) that the contribution of additional elements from chemical fertilizers or domestic/industrial wastewater to the Huanghe was minor and the fact that there are few tributaries in the downstream.

## 5. Conclusion

Mineralogy is the major factor controlling on the Mg isotope composition of suspended load. The dissolved Mg isotope composition throughout the Huanghe basin presents a wide range, from  $-1.53\%$  to  $-0.11\%$ . For the Huanghe main channel, the Mg isotope composition in the river water is less variable with most of the samples close to  $-1.09\%$ , and slightly decreases from upstream to downstream. Upstream of the Huanghe, the dissolved Mg isotopic composition was determined by the mixture of carbonate and silicate sources. Preferentially dissolution of minerals in loess is controlling the Mg isotope variation observed in downstream. The coherent decrease of Ca/Mg and  $\text{HCO}_3/\text{SO}_4$  or  $\text{HCO}_3/\text{Cl}$  favors the evaporite dissolution rather than carbonate weathering. In contrast, the  $\delta^{26}\text{Mg}$  values in the Huanghe main tributaries show a wide range. Evaporite dissolution and carbonate weathering was shown to be an important mechanism determining the Mg isotope composition in the tributaries. In addition, fractionation during secondary carbonate precipitation plays an important role on the Mg isotope composition of some tributaries. The low degree of biological activity in these rivers suggests that significant biological uptake of Mg is also unlikely. And also the influence from anthropogenic inputs is thought to be minor. Moreover, the strong relationships between

$\delta^{26}\text{Mg}$  and pH, temperature, and  $\delta^{18}\text{O}$  indicate that the Mg isotopic signature of river waters has the potential to serve as a good environmental indicator.

## Acknowledgments

The authors are grateful for Dr. E Tipper and an anonymous reviewer for their fruitful comments, as well as the suggestions from the Editor-in-chief, Jerome Gaillardet, which has greatly improved the earlier version of this paper. The authors thank Dr. B.L. Wang (Institute of Geochemistry, Chinese Academy of Sciences) for his thoughtful comments on an earlier version of the manuscript. This work was supported jointly by the Ministry of Science and Technology of China through the National Basic Research Program of China ('973' Program, Grant No. 2013CB956401); National Natural Science Foundation of China (Grant No. 41173030, 41372376, 41210004); and State Key Laboratory of Environmental Geochemistry (SKLEG2015408, SKLEG20120403).

## References

- Berner, E.K., Berner, R.A., 2012. *Global Environment: Water, Air, and Geochemical Cycles*, second ed. Princeton University Press, Princeton, New Jersey.
- Berner, R.A., Lasaga, A.C., Garrels, R.M., 1983. The carbonate-silicate geochemical cycle and its effect on atmospheric carbon dioxide over the past 100 million years. *Am. J. Sci.* 283, 641–683.
- Black, J.R., Epstein, E., Rains, W.D., Yin, Q.Z., Casey, W.H., 2008. Magnesium-isotope fractionation during plant growth. *Environ. Sci. Technol.* 42, 7831–7836.
- Black, J.R., Yin, Q.Z., Casey, W.H., 2006. An experimental study of magnesium-isotope fractionation in chlorophyll-A photosynthesis. *Geochim. Cosmochim. Acta* 70, 4072–4079.
- Bolou-Bi, E.B., Poszwa, A., Leyval, C., Vigier, N., 2010. Experimental determination of magnesium isotope fractionation during higher plant growth. *Geochim. Cosmochim. Acta* 74, 2523–2537.
- Brenot, A., Cloquet, C., Vigier, N., Carignan, J., France-Lanord, C., 2008. Magnesium isotope systematics of the lithologically varied Moselle river basin, France. *Geochim. Cosmochim. Acta* 72, 5070–5089.
- Buhl, D., Immenhauser, A., Smeulders, G., Kabiri, L., Richter, D.K., 2007. Time series  $\delta^{26}\text{Mg}$  analysis in speleothem calcite: kinetic versus equilibrium fractionation, comparison with other proxies and implications for palaeoclimate research. *Chem. Geol.* 244, 715–729.
- Buhl, D., Immenhauser, A., Richter, D., Schulte, U., Dietzel, M., Riechelmann, D., Niedermayr, A., 2009. Magnesium-isotope fractionation in a monitored limestone cave. *Geochim. Cosmochim. Acta* 73 A171–A171.
- Chang, V.T.C., Makishima, A., Belshaw, N.S., O'Nions, R.K., 2002. Purification of Mg from low-Mg biogenic carbonates for isotope ratio determination using multiple collector ICP-MS. *J. Anal. At. Spectrom.* 18, 296–301.
- Chen, J.S., Wang, F.Y., 2006. Geochemistry of water quality of the Yellow River basin. *Earth Sci. Front.* 13, 58–73 (in Chinese with English abstract).
- Dessert, C., Dupré, B., Gaillardet, J., François, L.M., Allegre, C.J., 2003. Basalt weathering laws and the impact of basalt weathering on the global carbon cycle. *Chem. Geol.* 202, 257–273.
- English, N.B., Quade, J., DeCelles, P.G., Garzzone, C.N., 2000. Geologic control of Sr and major element chemistry in Himalayan rivers, Nepal. *Geochim. Cosmochim. Acta* 64, 2549–2566.
- Fan, B.L., Zhao, Z.Q., Tao, F.X., Liu, B.J., Tao, Z.H., Gao, S., Zhang, L.H., 2014. Characteristics of carbonate, evaporite and silicate weathering in Huanghe River basin: a comparison among the upstream, midstream and downstream. *J. Asian Earth Sci.* 96, 17–26.
- Foster, G.L., Pogge von Strandmann, P.A.E., Rae, J.W.B., 2010. Boron and magnesium isotopic composition of seawater. *Geochem. Geophys. Geosyst.* 11.
- Galy, A., Bar-Matthews, M., Halicz, L., O'Nions, R.K., 2002. Mg isotopic composition of carbonate: insight from speleothem formation. *Earth Planet. Sci. Lett.* 201, 105–115.
- Geske, A., Goldstein, R.H., Mavromatis, V., Richter, D.K., Buhl, D., Kluge, T., John, C.M., Immenhauser, A., 2015a. The magnesium isotope ( $\delta^{26}\text{Mg}$ ) signature of dolomites. *Geochim. Cosmochim. Acta* 149, 131–151.
- Geske, A., Lokier, S., Dietzel, M., Richter, D.K., Buhl, D., Immenhauser, A., 2015b. Magnesium isotope composition of sabkha porewater and related (Sub-)recent stoichiometric dolomites, Abu Dhabi (UAE). *Chem. Geol.* 393–394, 112–124.
- Handler, M.R., Baker, J.A., Schiller, M., Bennett, V.C., Yaxley, G.M., 2009. Magnesium stable isotope composition of Earth's upper mantle. *Earth Planet. Sci. Lett.* 282, 306–313.
- Huang, K.J., Teng, F.Z., Elsenouy, A., Li, W.Y., Bao, Z.Y., 2013. Magnesium isotopic variations in loess: origins and implications. *Earth Planet. Sci. Lett.* 374, 60–70.
- Immenhauser, A., Buhl, D., Richter, D., Niedermayr, A., Riechelmann, D., Dietzel, M., Schulte, U., 2010. Magnesium-isotope fractionation during low-Mg calcite precipitation in a limestone cave – field study and experiments. *Geochim. Cosmochim. Acta* 74, 4346–4364.
- Jacobson, A.D., Blum, J.D., Walter, L.M., 2002. Reconciling the elemental and Sr isotope composition of Himalayan weathering fluxes: insights from the carbonate chemistry of stream waters. *Geochim. Cosmochim. Acta* 66, 3417–3429.
- Kisakurek, B., et al., 2009. Magnesium isotope fractionation in inorganic and biogenic calcite. *Geochim. Cosmochim. Acta* 73 A663.



- Kuhn, A.J., Schröder, W.H., Bauch, J., 2000. The kinetics of calcium and magnesium entry into mycorrhizal spruce roots. *Planta* 210, 488–496.
- Lee, S.W., Ryu, J.S., Lee, K.S., 2014. Magnesium isotope geochemistry in the Han River, South Korea. *Chem. Geol.* 364, 9–19.
- Li, W., Beard, B.L., Li, C., Xu, H., Johnson, C.M., 2015. Experimental calibration of mg isotope fractionation between dolomite and aqueous solution and its geological implications. *Geochim. Cosmochim. Acta* 157, 164–181.
- Li, W., Chakraborty, S., Beard, B.L., Romanek, C.S., Johnson, C.M., 2012. Magnesium isotope fractionation during precipitation of inorganic calcite under laboratory conditions. *Earth Planet. Sci. Lett.* 333–334, 304–316.
- Ling, M.X., Sedaghatpour, F., Teng, F.Z., Hays, P.D., Strauss, J., Sun, W., 2011. Homogeneous magnesium isotopic composition of seawater: an excellent geostandard for Mg isotope analysis. *Rapid Commun. Mass* 25, 2828–2836.
- Mavromatis, V., Gautier, Q., Bosc, O., Schott, J., 2013. Kinetics of Mg partition and Mg stable isotope fractionation during its incorporation in calcite. *Geochim. Cosmochim. Acta* 114, 188–203.
- Mavromatis, V., Meister, P., Oelkers, E.H., 2014a. Using stable Mg isotopes to distinguish dolomite formation mechanisms: a case study from the Peru margin. *Chem. Geol.* 385, 84–91.
- Mavromatis, V., Pearce, C.R., Shirokova, L., S., Bundeleva, I.A., Pokrovsky, O.S., Benezeth, P., Oelkers, E., H., 2012. Magnesium isotope fractionation during inorganic and cyanobacteria-induced hydrous magnesium carbonate precipitation. *Geochim. Cosmochim. Acta* 76, 161–174.
- Mavromatis, V., Prokushkin, A.S., Pokrovsky, O.S., Viers, J., Korets, M.A., 2014b. Magnesium isotopes in permafrost-dominated Central Siberian larch forest watersheds. *Geochim. Cosmochim. Acta* 147, 76–89.
- Meybeck, M., 1987. Global chemical weathering of surficial rocks estimated from river dissolved loads. *Am. J. Sci.* 287, 401–428.
- Noh, H., Huh, Y., Qin, J., Ellis, A., 2009. Chemical weathering in the Three Rivers region of Eastern Tibet. *Geochim. Cosmochim. Acta* 73, 1857–1877.
- Opfergelt, S., Burton, K.W., Georg, R.B., West, A.J., Guicharnaud, R.A., Sigfusson, B., Siebert, C., Gislason, S.R., Halliday, A.N., 2014. Magnesium retention on the soil exchange complex controlling Mg isotope variations in soils, soil solutions and vegetation in volcanic soils, Iceland. *Geochim. Cosmochim. Acta* 125, 110–130.
- Pogge von Strandmann, P.A.E., Burton, K.W., James, R.H., van Calsteren, P., Gislason, S., 2008a. The influence of weathering processes on riverine magnesium isotopes in a basaltic terrain. *Earth Planet. Sci. Lett.* 276, 187–197.
- Pogge von Strandmann, P.A.E., James, R.H., van Calsteren, P., Gislason, S.R., Burton, K.W., 2008b. Lithium, magnesium and uranium isotope behaviour in the estuarine environment of basaltic islands. *Earth Planet. Sci. Lett.* 274, 462–471.
- Ra, K., Kitagawa, H., 2007. Magnesium isotope analysis of different chlorophyll forms in marine phytoplankton using multi-collector ICP-MS. *J. Anal. Atom. Spectrom.* 22, 817–821.
- Ra, K., Kitagawa, H., Shiraiwa, Y., 2010. Mg isotopes in chlorophyll-A and coccoliths of cultured coccolithophores (*Emiliania huxleyi*) by MC-ICP-MS. *Mar. Chem.* 122, 130–137.
- Riechelmann, S., Buhl, D., Schröder-Ritzrau, A., Riechelmann, D.F.C., Richter, D.K., Vonhof, H.B., et al., 2012a. The magnesium isotope record of cave carbonate archives. *Clim. Past* 8, 1849–1867.
- Riechelmann, S., Buhl, D., Schroder-Ritzrau, A., Spötl, C., Riechelmann, D.F.C., et al., 2012b. Hydrogeochemistry and fractionation pathways of Mg isotopes in a continental weathering system: lessons from field experiments. *Chem. Geol.* 300, 109–122.
- Rudnick, R., Gao, S., 2003. Composition of the continental crust. *Treatise Geochem.* 3, 1–64.
- Rustad, J.R., Casey, W.H., Yin, Q.-Z., Bylaska, E.J., Felmy, A.R., Bogatko, S.A., Jackson, V.E., Dixon, D.A., 2010. Isotopic fractionation of  $Mg^{2+}$  (aq),  $Ca^{2+}$  (aq), and  $Fe^{2+}$  (aq) with carbonate minerals. *Geochim. Cosmochim. Acta* 74, 6301–6323.
- Saito, Y., Yang, Z., Hori, K., 2001. The Huanghe (Yellow River) and Changjiang (Yangtze River) deltas: a review on their characteristics, evolution and sediment discharge during the Holocene. *Geomorphology* 41, 219–231.
- Saulnier, S., Rollion-Bard, C., Vigier, N., Chaussidon, M., 2012. Mg isotope fractionation during calcite precipitation: an experimental study. *Geochim. Cosmochim. Acta* 91, 75–91.
- Schauble, E.A., 2011. First-principles estimates of equilibrium magnesium isotope fractionation in silicate, oxide, carbonate and hexaaquamagnesium(2+) crystals. *Geochim. Cosmochim. Acta* 75, 844–869.
- Schmitt, A.D., Vigier, N., Lemarchand, D., Millot, R., Stille, P., Chabaux, F., 2012. Processes controlling the stable isotope compositions of Li, B, Mg and Ca in plants, soils and waters: a review. *Compt. Rendus Geosci.* 344, 704–722.
- Shirokova, L., Mavromatis, V., Bundeleva, I., Pokrovsky, O., Bénéthet, P., Gérard, E., Pearce, C., Oelkers, E., 2013. Using Mg isotopes to trace cyanobacterially mediated magnesium carbonate precipitation in alkaline lakes. *Aquat. Geochem.* 19, 1–24.
- Teng, F.Z., Li, W.Y., Ke, S., Marty, B., Dauphas, N., Huang, S., Wu, F.Y., Pourmand, A., 2010. Magnesium isotopic composition of the Earth and chondrites. *Geochim. Cosmochim. Acta* 74, 4150–4166.
- Teng, F.Z., Wadhwa, M., Helz, R.T., 2007. Investigation of magnesium isotope fractionation during basalt differentiation: implications for a chondritic composition of the terrestrial mantle. *Earth Planet. Sci. Lett.* 261, 84–92.
- Tipper, E.T., Calmels, D., Gaillardet, J., Louvat, P., Capmas, F., Dubacq, B., 2012a. Positive correlation between Li and Mg isotope ratios in the river waters of the Mackenzie Basin challenges the interpretation of apparent isotopic fractionation during weathering. *Earth Planet. Sci. Lett.* 333, 35–45.
- Tipper, E.T., Gaillardet, J., Louvat, P., Capmas, F., White, A.F., 2010. Mg isotope constraints on soil pore-fluid chemistry: evidence from Santa Cruz, California. *Geochim. Cosmochim. Acta* 74, 3883–3896.
- Tipper, E.T., Galy, A., Bickle, M.J., 2006a. Riverine evidence for a fractionated reservoir of Ca and Mg on the continents: implications for the oceanic Ca cycle. *Earth Planet. Sci. Lett.* 247, 267–279.
- Tipper, E.T., Galy, A., Bickle, M.J., 2008. Calcium and magnesium isotope systematics in rivers draining the Himalaya-Tibetan-Plateau region: Lithological or fractionation control? *Geochim. Cosmochim. Acta* 72, 1057–1075.
- Tipper, E.T., Galy, A., Gaillardet, J., Bickle, M.J., Elderfield, H., Carder, E.A., 2006b. The magnesium isotope budget of the modern ocean: constraints from riverine magnesium isotope ratios. *Earth Planet. Sci. Lett.* 250, 241–253.
- Tipper, E.T., Lemarchand, E., Hindshaw, R.S., Reynolds, B.C., Bourdon, B., 2012b. Seasonal sensitivity of weathering processes: hints from magnesium isotopes in a glacial stream. *Chem. Geol.* 312, 80–92.
- de Villiers, S., Dickson, J.A.D., Ellam, R.M., 2005. The composition of the continental river weathering flux deduced from seawater Mg isotopes. *Chem. Geol.* 216, 133–142.
- Wang, B., Lee, X.Q., Yuan, H.L., Zhou, H., Cheng, H.G., Cheng, J.Z., Zhou, Z.H., Xing, Y., Fang, B., Zhang, L.K., 2012. Distinct patterns of chemical weathering in the drainage basins of the Huanghe and Xijiang River, China: evidence from chemical and Sr-isotopic compositions. *J. Asian Earth Sci.* 59, 219–230.
- Wimpenny, J., Burton, K.W., James, R.H., Gannoun, A., Mokadem, F., Gislason, S.R., 2011. The behaviour of magnesium and its isotopes during glacial weathering in an ancient shield terrain in West Greenland. *Earth Planet. Sci. Lett.* 304, 260–269.
- Wimpenny, J., Colla, C.A., Yin, Q.Z., Rustad, J.R., Casey, W.H., 2014a. Investigating the behaviour of Mg isotopes during the formation of clay minerals. *Geochim. Cosmochim. Acta* 128, 178–194.
- Wimpenny, J., Gislason, S.R., James, R.H., Gannoun, A., Pogge Von Strandmann, P.A.E., Burton, K.W., 2010. The behaviour of Li and Mg isotopes during primary phase dissolution and secondary mineral formation in basalt. *Geochim. Cosmochim. Acta* 74, 5259–5279.
- Wimpenny, J., Yin, Q.Z., Tollstrup, D., Xie, L.W., Sun, J., 2014b. Using Mg isotope ratios to trace Cenozoic weathering changes: a case study from the Chinese Loess Plateau. *Chem. Geol.* 376, 31–43.
- Wu, L., Huh, Y., Qin, J., Du, G., van Der Lee, S., 2005. Chemical weathering in the Upper Huang He (Yellow River) draining the eastern Qinghai-Tibet Plateau. *Geochim. Cosmochim. Acta* 69, 5279–5294.
- Yokoo, Y., Nakano, T., Nishikawa, M., Quan, H., 2004. Mineralogical variation of Sr-Nd isotopic and elemental compositions in loess and desert sand from the central Loess Plateau in China as a provenance tracer of wet and dry deposition in the northwestern Pacific. *Chem. Geol.* 204, 45–62.
- Young, E.D., Galy, A., 2004. The isotope geochemistry and cosmochemistry of magnesium. *Rev. Mineral. Geochem.* 55, 197–230.
- Zhang, J., Huang, W., Letolle, R., Jusserand, C., 1995. Major element chemistry of the Huanghe (Yellow River), China-weathering processes and chemical fluxes. *J. Hydrol.* 168, 173–203.
- Zhang, J., Huang, W.W., Liu, M.G., Zhou, Q., 1990. Drainage basin weathering and major element transport of two large Chinese rivers (Huanghe and Changjiang). *J. Geophys. Res.* 95, 13277–13288.